Iron-sulfur cluster repair contributes to *Y. pseudotuberculosis* survival within deep tissues.

Running title: Iron-sulfur cluster repair during *Y. pseudotuberculosis* infection

Kimberly M. Davis[1,#a,*], Joanna Krupp[1], Stacie Clark[1,2], Ralph R. Isberg[1]

[1]Department of Molecular Biology and Microbiology
[2]Graduate Program in Molecular Microbiology, Sackler School of Graduate Biomedical Science
Tufts University School of Medicine, Boston, MA, USA
[#a]Current Address: W. Harry Feinstone Department of Molecular Microbiology and Immunology
Johns Hopkins Bloomberg School of Public Health, Baltimore, MD, USA

*Corresponding author:

E-mail: kdavi140@jhu.edu (KMD)

Abstract

To successfully colonize host tissues, bacteria must respond to and detoxify many different host-derived antimicrobial compounds, such as nitric oxide (NO). NO can directly kill bacteria, primarily through attack on iron-sulfur (Fe-S) cluster-containing proteins. NO detoxification plays an important role in promoting bacterial survival, but it remains unclear if repair of Fe-S clusters is also important for bacterial survival within host tissues. Here we show that the Fe-S cluster repair protein, YtfE, contributes to the survival of *Y. pseudotuberculosis* within the spleen following nitrosative stress. *Y. pseudotuberculosis* forms clustered centers of replicating bacteria within deep tissues, where peripheral bacteria express the NO-detoxifying gene, *hmp*. *ytfE* expression also occurred specifically within peripheral cells at the edges of microcolonies. In the absence of *ytfE*, the area of microcolonies was significantly smaller than WT, consistent with *ytfE* contributing to the survival of peripheral cells. The loss of *ytfE* did not alter the ability of cells to detoxify NO, which occurred within peripheral cells in both WT and Δ*ytfE* microcolonies. In the absence of NO-detoxifying activity by *hmp*, NO diffused across Δ*ytfE* microcolonies, and there was a significant decrease in the area of microcolonies lacking *ytfE*, indicating that *ytfE* also contributes to bacterial survival in the absence of NO detoxification. These results indicate a role for Fe-S cluster repair in the survival of *Y. pseudotuberculosis* within the spleen, and suggest that extracellular bacteria may rely on this pathway for survival within host tissues.

43 **Introduction**

44 Nitric oxide (NO) is a diffusible gas that has a wide range of physiological functions
45 within mammals (1, 2). The effects of NO are tissue concentration-dependent, as it promotes
46 vasodilation, cell proliferation and cell differentiation at low concentrations (3, 4), while high
47 concentrations drive apoptosis and defense against bacterial, fungi, and parasites (5-8). NO is
48 produced by three different nitric oxide synthase (NOS) isoforms within mammalian tissues: the
49 neuronal NOS (nNOS), endothelial NOS (eNOS), and inducible NOS (iNOS). nNOS and eNOS
50 are expressed at low levels by endothelial and neuronal cells respectively (2). In contrast, iNOS
51 is expressed by a wide range of cell types, specifically in response to NF-κB-dependent sensing
52 of, and is responsible for the high levels of NO produced during infection (1, 9).

53 NO has direct bactericidal activity and can also react with reactive oxygen species to
54 produce additional toxic compounds. NO antibacterial activity occurs primarily through
55 nitrosylation of iron-sulfur (Fe-S) cluster-containing proteins, which play critical roles in cellular
56 respiration, DNA synthesis, and gene regulation. One of the global regulators in *E. coli* that has
57 been shown to be inactivated by NO is NsrR (10), which regulates the response to nitrosative
58 stress and is also associated with the oxidative stress response (11-13). Nitrosylation of the
59 NsrR-associated Fe-S cluster relieves repression of at least 60 genes in *E. coli* (14-17). Included
60 in this regulon is the *hmp* gene, which encodes a flavohemoglobin that detoxifies NO (18, 19),
61 and YtfE (also known as Repair of Iron Centers (RIC) in *E. coli*), which functions to repair Fe-S
62 clusters following NO damage (12, 16). Repair of Fe-S cluster proteins by YtfE can eliminate the
63 need for new Fe-S cluster biogenesis when Fe availability is limited (12, 20, 21). A variety of
64 studies argue that YtfE contributes to bacterial survival within host cells, but it remains unclear if

65 YtfE contributes to the survival of extracellular pathogens replicating within host tissues, and if
66 YtfE contributes to survival following exposure to NO (22-24).

67 *Yersinia pseudotuberculosis* is an oral pathogen that is typically contained within
68 intestinal tissues and gut-associated lymphoid tissues, but has the capacity to spread systemically
69 in susceptible individuals (25-28). Following bloodstream access, *Y. pseudotuberculosis*
70 colonizes deep tissue sites where individual bacteria replicate to form clonal microcolonies (29-
71 31). Neutrophils, monocytes, and macrophages are recruited to sites of bacterial replication,
72 which are kept at bay by *Yersinia*, primarily via substrates of the bacterial type III secretion
73 system (32-34). Recruited monocytes and macrophages produce NO, which diffuses across a
74 layer of neutrophils and is inactivated at the periphery of the microcolony by bacteria expressing
75 Hmp, preventing diffusion of NO into the interior of the microcolony (31). The consequences of
76 the selective attack of NO on the peripheral bacteria are unclear, although it is likely that
77 nitrosative stress may slow their growth. Additional members of the nitrosative stress response,
78 such as YtfE, may also be required in peripheral cells to ensure their survival.

79 Bacteria responding to RNS appear to recover and remain viable, consistent with
80 members of the NsrR regulon cooperating to repair NO-mediated damage in peripheral bacteria
81 within microcolonies. Two of the members of the *E. coli* NsrR regulon, *hmp* and *ytfE,* are
82 upregulated in the bubonic plague model of *Yersinia pestis* infection (35), so *ytfE* is likely a
83 member of the NsrR regulon in *Yersinia* and could contribute to microbial fitness during
84 microcolony growth. Additionally, very few studies have explored the role of Fe-S cluster repair
85 during infection with extracellular bacteria. Here, we show that *ytfE* contributes to the survival
86 of extracellular bacteria, specifically through upregulation of *ytfE* within peripheral cells of *Y.*
87 *pseudotuberculosis* microcolonies.

88 **Results.**

89 ***Y. pseudotuberculosis ytfE* expression is regulated by NsrR and occurs within peripheral**
90 **cells during growth in the spleen.**

91 The *ytfE* gene is known to be a member of the NsrR regulon in a number of bacterial
92 species (12, 13, 36), so *ytfE* is expected to be repressed by NsrR in *Y. pseudotuberculosis*. We
93 also expected that *ytfE* is transcribed during *Y. pseudotuberculosis* growth within the mouse
94 spleen as dthe NsrR-regulated *hmp* gene is expressed in this tissue (22-24, 31, 35). To determine
95 if *Y. pseudotuberculosis ytfE* is expressed during splenic growth, C57BL/6 mice were
96 intravenously challenged with bacteria and bacterial RNA was isolated at day 3 post-inoculation
97 (PI). Based on qRT-PCR analysis, *ytfE* transcript levels increased within the mouse spleen
98 relative to the inoculum culture grown in the absence of an NO-generating system, with marked
99 mouse-to-mouse variation (Figure 1A) (31). To determine if *ytfE* expression is NsrR-dependent,
100 we compared *ytfE* transcription levels in WT and Δ*nsrR* strains in the presence (+) and absence (-)
101 of nitrogen stress imparted by acidified nitrite (NO_2). Transcription of *ytfE* increased by over
102 100X in the WT strain with the addition of nitrogen stress (Figure 1B). As expected, transcription
103 of *ytfE* was high in the Δ*nsrR* strain in either the presence or absence of nitrogen stress, indicating
104 that NsrR negatively regulates *ytfE* transcription.

105 Hmp, another member of the NsrR regulon, is specifically expressed on the periphery of
106 *Y. pseudotuberculosis* microcolonies during splenic growth (31). At the transcriptional level,
107 this is associated with considerable variation in expression levels between individual mice. The
108 variable *ytfE* expression levels in the mouse and NsrR-dependence is reminiscent of *hmp*
109 expression, indicating that there could be a link between spatial expression and inter-mouse
110 variation. To determine if *ytfE* and *hmp* have similar expression patterns during growth in the

111 spleen, mice were intravenously inoculated with a WT *Y. pseudotuberculosis* strain containing
112 *hmp::mCherry* (chromosomal integration of *mCherry* downstream of *hmp*) and *ytfE::gfp*
113 (chromosomal integration of *gfp* downstream of *ytfE*). Microcolonies were visualized within the
114 spleen using fluorescence microscopy, and *ytfE* and *hmp* reporter signals were quantified within
115 the same cells at the center and periphery of the microcolonies (Materials and Methods). The
116 *hmp* reporter signal increased within individual cells at the periphery relative to cells at the
117 centroid of microcolonies, which generated a ratio value greater than 1, consistent with *hmp*
118 peripheral expression (Figure 1C). The *ytfE* signal was dim relative to *hmp*, but also increased at
119 the periphery of microcolonies relative to the centroid. The Periphery/Centroid signal intensity
120 ratio value for *ytfE* was similar to *hmp*, indicating that *ytfE* was expressed at the periphery of
121 microcolonies (Figure 1C). There was significant overlap in the *hmp* and *ytfE* signals within
122 these images, and based on NsrR-dependent regulation of both genes, it is likely that *hmp* and
123 *ytfE* were expressed in the same cells (Figure 1D).

124 ***ytfE* contributes to the virulence of *Y. pseudotuberculosis* in the spleen.**

125 YtfE repairs Fe-S clusters damaged by NO, and there appears to be sufficient NO at the
126 periphery of splenic microcolonies to allow synthesis of this protein and to promote repair within
127 this subpopulation of bacteria. To determine if loss of *yftE* alters the overall fitness of *Y.*
128 *pseudotuberculosis* during growth within the spleen, we constructed a *Y. pseudotuberculosis*
129 strain that lacks the *ytfE* gene (Δ*ytfE*) and harbors a constitutive *gfp*-expressing plasmid, to
130 visualize growth within the spleen. To compare differences in relative fitness, mice were
131 infected intravenously with equal amounts of WT mCherry$^+$ and Δ*ytfE* GFP$^+$ strains, and spleens
132 were harvested at day 3 PI to determine the competitive index by colony forming units (CFUs)
133 and quantify microcolony areas within the same animals. At day 3 PI, the median competitive

134 index was less than 1, indicating lowered fitness of the Δ*ytfE* strain relative to the WT strain
135 (Figure 2A). The areas of individual microcolonies within these tissues were also visualized and
136 quantified by fluorescence microscopy. In addition, the Δ*ytfE* microcolonies were significantly
137 smaller than WT microcolonies within the same organs, indicating that *ytfE* contributes to the
138 survival of *Y. pseudotuberculosis* in the spleen, presumably due to lowered fitness of the
139 bacterial population located at the periphery of the microcolonies (Figure 2B).
140 Since YtfE could directly repair the Fe-S cluster of NsrR, the absence of *ytfE* could alter
141 expression of the NsrR regulon, by resulting in heightened expression within peripheral cells. To
142 determine if microcolonies from the *Y. pseudotuberculosis* Δ*ytfE* strain have sustained
143 expression of the NsrR regulon relative to the WT strain, we infected mice intravenously with
144 WT GFP^+ *hmp::mCherry* or Δ*ytfE* GFP^+ *hmp::mCherry* integrated *hmp* reporter strains, and
145 spleens were harvested at day 3 PI to visualize reporter expression by fluorescence microscopy.
146 Similar to Fig. 1D, *hmp* reporter expression was significantly higher at the periphery relative to
147 the centroid in the WT strain (Figure 2C). The reporter expression pattern was very similar in
148 Δ*ytfE* microcolonies, indicating that there was still a gradient of NO exposure in the mutant, in
149 which Hmp activity in the peripheral population protects the central population of bacteria, and
150 that loss of *ytfE* did not significantly alter expression of the NsrR regulon (Figure 2D).
151 **Loss of *ytfE* and *hmp* reduces *Y. pseudotuberculosis* fitness.**
152 YftE contributed to the growth of *Y. pseudotuberculosis* microcolonies in the spleen
153 despite expression limited to the microcolony periphery. We were then interested in determining
154 if YtfE-mediated repair played an important role in the context of a Δ*hmp* strain, where all
155 bacteria in a microcolony are exposed to NO (31). We first compared the virulence of WT and
156 Δ*hmp* Δ*ytfE* microcolonies during single strain infection. Mice were infected intravenously with

157 WT GFP$^+$ or Δ*hmp* Δ*ytfE* GFP$^+$ strains, and spleens were harvested at day 3 PI to visualize
158 microcolony areas by fluorescence microscopy. Individual Δ*hmp* Δ*ytfE* microcolonies were
159 significantly smaller than WT, consistent with impaired growth of the Δ*hmp* Δ*ytfE* strain (Figure
160 3A). We also determined the relative fitness of the WT and Δ*hmp* Δ*ytfE* strains by comparing
161 growth within the same tissue during co-infection. Mice were infected intravenously with WT
162 mCherry$^+$ and Δ*hmp* Δ*ytfE* GFP$^+$ strains, and spleens were harvested at day 3 PI to quantify
163 CFUs and visualize microcolony areas by fluorescence microscopy. The median competitive
164 index value was below 1, indicating that the Δ*hmp* Δ*ytfE* strain had reduced fitness relative to the
165 WT strain (Figure 3B). The microcolony areas of the Δ*hmp* Δ*ytfE* were also significantly smaller
166 than WT microcolonies, indicating the Δ*hmp* Δ*ytfE* had reduced fitness in the spleen relative to
167 the WT strain (Figure 3C).

168 ***ytfE* contributes to bacterial survival in the absence of *hmp*.**

169 As the fitness of the Δ*ytfE* or Δ*hmp* Δ*ytfE* strains showed similar defects when compared
170 to WT (Figure 3), it is not clear if YftE contributes to *Y. pseudotuberculosis* colonization of the
171 spleen in the absence of Hmp function. To address this point, we challenged mice intravenously
172 with Δ*hmp* GFP$^+$ P_{hmp}*::mCherry* and Δ*hmp* Δ*ytfE* GFP$^+$ P_{hmp}*::mCherry* strains, and spleens were
173 harvested at day 3 PI to quantify CFUs, visualize microcolony areas, and detect reporter signals
174 by fluorescence microscopy. The median competitive index (CI) value for the double mutant
175 was below 1, indicating that Δ*hmp* Δ*ytfE* strain was less fit than Δ*hmp* (Figure 4A).
176 Interestingly, in 4 mice the CI was at least 1, indicating that the Δ*hmp* Δ*ytfE* strain could compete
177 efficiently with Δ*hmp* in these animals. We then compared the total CFU in the organs in mice
178 in which the Δ*hmp* strain outcompeted Δ*hmp* Δ*ytfE*, or in mice in which no such outcompetition
179 took place (Figure 4B). The total CFUs were significantly lower in organs in which the Δ*hmp*

180 did not outcompete the Δ*hmp*Δ*ytfE* strain, indicating that the fitness differences were suppressed
181 in animals showing increased restriction of bacterial growth. The microcolony areas were
182 quantified within all the spleens depicted in Figure 4A, and the areas of Δ*hmp* Δ*ytfE*
183 microcolonies were significantly smaller than Δ*hmp* (Figure 4C). Δ*hmp* Δ*ytfE* microcolonies had
184 similar P_{hmp} reporter expression at the centroid and periphery, indicating NO diffused across
185 these centers (Figure 4D). Together, these results confirm that *ytfE* contributes to bacterial
186 survival in the absence of Hmp detoxifying activity.

187 ***ytfE* has limited effects on NO sensitivity in the absence of *hmp***

188 The Δ*ytfE* single mutant strain had reduced fitness relative to the WT strain (Figure 2),
189 however the single Δ*ytfE* mutant was not significantly more sensitive than the WT strain to the
190 presence of acidified nitrite during growth in culture.:. Similarly, despite the lowered fitness of
191 the Δ*hmp* Δ*ytfE* strain in spleens relative to Δ*hmp*, the Δ*hmp* Δ*ytfE* strain was not significantly
192 more sensitive than the Δ*hmp* mutant strain to the presence of acidified nitrite during growth in
193 culture (Figure 5A; compare +NO_2 samples). This is consistent with previous reports in other
194 organisms (36, 37), perhaps due to the presence of other backup repair pathways that are active
195 in the absence of Hmp or because YftE plays a role in protection from other stress species.

196 We then compared *hmp* reporter expression in Δ*ytfE* and Δ*hmp*Δ*ytfE* strains to confirm
197 that NO diffusion occurred across Δ*hmp* Δ*ytfE* microcolonies using plasmid-borne reporters.
198 Mice were infected intravenously with Δ*ytfE* GFP^+ P_{hmp}*::mCherry* or Δ*hmp* Δ*ytfE* GFP^+
199 P_{hmp}*::mCherry* strains, and spleens were harvested 3 days PI to visualize reporter expression by
200 fluorescence microscopy. The Δ*ytfE* strain had peripheral P_{hmp} reporter expression, as seen with
201 the chromosomally-integrated *hmp* reporter, indicating that NO diffusion across the microcolony
202 is inhibited by peripheral cells in Δ*ytfE* microcolonies (Figure 5B, 5C). Δ*hmp* Δ*ytfE*

203 microcolonies showed no such preference for the periphery, indicating NO diffused across these
204 centers, as expected based on the loss of *hmp*.

205 **Rescue of *ytfE* restores microcolony size.**

206 To show that the loss of *ytfE* was responsible for decreased microcolony size, we rescued
207 the Δ*ytfE* strain with a WT copy of *ytfE*, and transformed the *ytfE* rescued strain with the
208 constitutive *gfp*-expressing plasmid. Mice were infected intravenously with WT mCherry$^+$ and
209 *ytfE* rescued GFP$^+$ strains, and spleens were harvested at day 3 PI to quantify CFUs and visualize
210 microcolony areas by fluorescence microscopy. The median competitive index for the *ytfE*
211 rescued strain was close to a value of 1, indicating the fitness of this strain was roughly
212 equivalent to the WT strain (Figure 6A). The microcolony areas were quantified within all the
213 spleens depicted in Figure 6A, and the areas of *ytfE* rescued microcolonies were very similar to
214 WT microcolonies (Figure 6B, 6C). These results indicate that the Δ*ytfE* strain was rescued by
215 the WT copy of *ytfE*, which confirms that the reduced fitness of the Δ*ytfE* strain was specifically
216 due to a loss of *ytfE*.

217 **Discussion**

218 The detoxification of NO and other reactive nitrogen species is critical for bacterial
219 survival within host tissues (38-41). Bacterial proteins involved in NO detoxification, however,
220 are not synthesized until NO accumulates and damages the Fe-S clusters of NsrR, resulting in
221 inactivation of this repressor (14, 15). Many additional Fe-S cluster-containing proteins are
222 simultaneously damaged, so bacteria need to either repair damaged proteins or synthesize
223 replacement proteins, while simultaneously replenishing proteins that detoxify NO and prevent
224 further damage (16, 36). Although Fe-S cluster repair is likely required for bacterial survival, it
225 has been unclear whether or not this plays an important role within host tissues. We have chosen
226 to ask this question in a mouse model of *Y. pseudotuberculosis* infection, where it is known that
227 bacteria respond to RNS and that Fe concentrations are limiting (23, 24, 31). Here, we have
228 shown that Fe-S cluster repair contributes to successful *Y. pseudotuberculosis* replication within
229 the spleen.

230 We found that a place where Fe-S cluster repair in *Y. pseudotuberculosis* likely occurs is
231 in the peripheral subpopulation of bacteria that responds to NO assault within microcolonies.
232 This is consistent with a role for YftE in supporting survival of the peripheral subpopulation. In
233 the absence of *ytfE*, we would expect bacteria on the periphery to be exposed to stress associated
234 with NO exposure, leading to sequential loss of the peripheral population and progressively
235 smaller microcolonies. Consistent with this hypothesis, we observed Δ*ytfE* microcolonies were
236 smaller than those established by the WT strain. It is expected that the difference between WT
237 and Δ*ytfE* microcolony areas will become progressively more pronounced as the infection
238 proceeds, because Δ*ytfE* microcolonies should continuously lose their peripheral subpopulation.
239 This prediction is based on our previous observation that NO-sensitive microcolonies are

240 progressively reduced during the course of disease, with elimination of Δ*hmp* bacteria by NO
241 most pronounced at late timepoints post-inoculation, concurrent with a timepoint in which the
242 animals inoculated with the WT strain are moribund (PI).

243 NO alone was not sufficient to limit the growth of Δ*ytfE* bacteria in bacteriological
244 media, consistent with previous studies that indicated the uropathogenic *E. coli* (UPEC) Δ*ytfE*
245 strain had reduced intracellular survival within host cells, but was not sensitive to exogenous NO
246 alone (37). Presumably, the Δ*ytfE* strain is sensitive to other antimicrobial compounds generated
247 within host tissues, possibly by the generation of a variety of reactive nitrogen species (RNS) as
248 a consequence of NO reaction with reactive oxygen species (ROS) or other compounds.
249 Upregulation of *ytfE* following hydrogen peroxide-mediated damage of *Staphylococcus aureus*
250 indicates that YtfE plays a broad role in repair, instead of just a response to nitrogen stress (42).

251 An additional regulatory signal for the *yftE* gene is iron limitation, which depresses
252 synthesis of new Fe-S cluster proteins, thus requiring cellular YftE function (13, 20, 43). The
253 spleen is expected to be an iron-limiting environment requiring Fe-S cluster repair, but we found
254 no evidence for NO-independent induction of the *ytfE* gene within the center of microcolonies,
255 using our fluorescent promoter constructions. This contrasts with data arguing that *Y.*
256 *pseudotuberculosis* expresses many Fe acquisition genes during growth in host tissues, consistent
257 with Fe-limiting conditions within host tissues (24, 44). It is possible that the center of the
258 microcolony represents a protected environment with low exposure to stresses such as reactive
259 nitrogen and oxygen species as well as limited damage to Fe-S centers. Additionally, *ytfE*
260 expression may be induced at very low NO concentrations, as seen in *Salmonella enterica*
261 serovar Typhimurium (36), but may require severe iron limitation for expression in the absence
262 of NO.

263 The loss of YftE function also has the potential to alter metabolite levels due to
264 disruption of protein functions that are Fe-S center-related. In the presence of RNS, a Δ*ytfE*
265 strain may have reduced aconitase and fumarase activity due to the role of YtfE in Fe-S cluster
266 repair specifically for these proteins (45). The Fe-S cluster of the NsrR repressor is also repaired
267 by YtfE, which could lead to prolonged expression of the NsrR regulon in the presence of NO
268 (12). Our results indicate that expression of the NsrR regulon is similar in the presence or
269 absence of *ytfE*, although it remains possible that prolonged expression of the NsrR regulon
270 could be detected at later timepoints post-inoculation. Future work will investigate these issues,
271 and determine the interplay between iron regulation, NO-induced damage and repair of critical
272 Fe-S centers.

273 **Materials and Methods**

274 *Bacterial strains & growth conditions.* The WT *Y. pseudotuberculosis* strain, YPIII, was
275 used throughout. For all mouse infection experiments, bacteria were grown overnight to post-
276 exponential phase in 2xYT broth (LB, with 2x yeast extract and tryptone) at 26° C with rotation.
277 Exponential phase cultures were sub-cultured 1:100 from overnight cultures, and grown at 26° C
278 with rotation for an additional 2 hours. Sodium nitrite (2.5mM) was added to LB pH5.5 to
279 induce the nitrogen stress response.

280 *Generation of ytfE mutant strains.* The *hmp* and *nsrR* deletion strains were previously
281 described (31). Deletion derivative strains were generated for *ytfE* by amplifying the start codon
282 + 3 downstream codons, the 3' terminal 3 codons + the stop codon and fusing these fragments to
283 generate a start + 6 aa + stop construct. Deletion constructions were amplified with 500 base
284 pairs flanking sequence on each side, cloned into the suicide vector, pSR47S, and transformed
285 into *Y. pseudotuberculosis*. Sucrose selection was used to select for bacteria that had
286 incorporated the desired mutation after a second cycle of recombination (30). PCR, sequencing,
287 and qRT-PCR were used to confirm deletion strains.

288 *Integrated ytfE reporter construction (ytfE^{+}rescue strain).* The *ytfE::gfp* reporter was
289 generated by cloning *gfp* immediately downstream of the *ytfE* gene (in between the *ytfE* stop
290 codon and terminator sequence) by overlap extension PCR. The *ytfE* start codon was amplified
291 with 500 base pairs upstream flanking sequence, while the stop codon of *gfp* was amplified with
292 500 base pairs downstream flanking sequence. This fragment was cloned into the suicide vector,
293 pSR47S, and transferred by conjugation into WT *Y. pseudotuberculosis hmp::mCherry*
294 (chromosomally integrated), selecting for kanamycin resistance. For the *ytfE*$^{+}$ rescue strain, a
295 WT *ytfE* gene product, including 500 base pairs upstream and downstream of *ytfE*, was amplified

296 from genomic DNA and cloned into pSR47S. This vector was transferred by conjugation into
297 Δ*ytfE Y. pseudotuberculosis*, selecting for kanamycin resistance. A second round of
298 recombination was selected on sucrose-containing media to isolate strains that had recombined
299 each *ytfE* construct. PCR and sequencing were used to confirm integration of *gfp* or rescue of
300 the *ytfE* deletion.

301 *Generation of plasmid-based reporter strains.* Several of the *Y. pseudotuberculosis*
302 reporter strains in this study have been previously described: WT GFP^+, WT $mCherry^+$
303 (*yopE::mCherry)*, WT *hmp::mCherry*, WT GFP^+ *hmp::mCherry*, and Δ*hmp* GFP^+ (31). For this
304 study, GFP^+ strains were constructed by transforming deletion strains with the constitutive GFP
305 plasmid, which expresses GFP from an unrepressed P_{tet} of pACYC184. The P_{hmp}*::mCherry* was
306 also transformed into GFP^+ strains. The P_{hmp}*::mCherry* transcriptional fusion was previously
307 constructed by fusing the *hmp* promoter to *mCherry* using overlap extension PCR, and cloned
308 into the pMMB67EH plasmid (31).

309 *Murine model of systemic infection.* Six to 8-week old female C57BL/6 mice were
310 obtained from Jackson Laboratories (Bar Harbor, ME). All animal studies were approved by the
311 Institutional Animal Care and Use Committee of Tufts University. Mice were injected
312 intravenously with 10^3 bacteria for all experiments. For co-infection experiments, mice were
313 inoculated with 5 x 10^2 CFU of each strain, for a total of 10^3 CFUs. At the indicated timepoints
314 post-inoculation (PI) (3 days), spleens were removed and processed.

315 *qRT-PCR to detect bacterial transcripts in broth-grown cultures.* Bacterial cells were
316 grown in broth to A_{600} = 0.3 under appropriate stress conditions, pelleted, resuspended in Buffer
317 RLT (QIAGEN) + ß-mercaptoethanol, and RNA was isolated using the RNeasy kit (QIAGEN)
318 according to manufacturer's protocol. DNA contamination was eliminated using the DNA-free

319 kit (Ambion) according to manufacturer's protocol. RNA was reverse transcribed using M-MLV
320 reverse transcriptase (Invitrogen), in the presence of the RNase inhibitor, RnaseOUT
321 (Invitrogen), according to manufacturer's protocol. Approximately 30 ng cDNA was used as a
322 template in reactions with 0.5 μM of forward and reverse primers and SYBR Green (Applied
323 Biosystems) according to manufacturer's protocol. Control samples were prepared that lacked
324 M-MLV, to confirm DNA was eliminated from samples and was not amplified by qRT-PCR.
325 Reactions were carried out using the StepOnePlus Real-Time PCR system, and relative
326 comparisons were obtained using the $\Delta\Delta C_T$ or $2^{-\Delta Ct}$ method (Applied Biosystems).
327 *qRT-PCR to detect bacterial transcripts from mouse tissues.* Mice were inoculated
328 intravenously with the WT strain, and at day 3 PI spleens were harvested, and immediately
329 submerged in RNALater solution (QIAGEN). Tissue was homogenized in Buffer RLT + ß-
330 mercaptoethanol, and RNA was isolated using the RNeasy kit (QIAGEN) according to
331 manufacturer's protocol. Bacterial RNA was enriched following depletion of host mRNA and
332 rRNA from total RNA samples, using the MICROB*Enrich* kit (Ambion) according to
333 manufacturer's protocol. DNA digestion, reverse transcription, and qRT-PCR were performed
334 as described above.
335 *Fluorescence microscopy.* C57BL/6 mice were inoculated intravenously with the *Y.*
336 *pseudotuberculosis* WT strain, at day 3 PI spleens were harvested and immediately fixed in 4%
337 paraformaldehyde in PBS for 3 hours. Tissues were frozen-embedded in Sub Xero freezing
338 media (Mercedes Medical) and cut by cryostat microtome into 10μm sections. To visualize
339 reporters, sections were thawed in PBS, stained with Hoechst at a 1:10,000 dilution, washed in
340 PBS, and coverslips were mounted using ProLong Gold (Life Technologies). Tissue was imaged
341 with 20x or 63x objectives, using a Zeiss Axio Observer.Z1 (Zeiss) fluorescent microscope with

342 Colibri.2 LED light source, an Apotome.2 (Zeiss) for optical sectioning, and an ORCA-R^2 digital
343 CCD camera (Hamamatsu).
344
345 *Image analysis.* Volocity image analysis software was used to quantify microcolony
346 areas. Image J was used to quantify the signal intensity of each channel at the centroid and
347 periphery of each microcolony, to generate relative signal intensities of fluorescent reporters.
348 Thresholding was used to define the area of each microcolony, the centroid was calculated, and
349 0.01 $pixel^2$ squares were selected to calculate values at the centroid. Peripheral measurements
350 depict bacteria in contact with host cells.
351
352 **Author Contributions.** Designed and performed experiments: KMD, JK, SC.
353 Intellectual/conceptual contribution: KMD, RRI. Analyzed the data: KMD, JK, SC, RRI. Wrote
354 the paper: KMD, RRI.
355
356 **Acknowledgments.** We thank the members of the Isberg lab, who provided valuable
357 advice and feedback throughout this project. We also thank the members of the Davis lab, who
358 provided feedback and suggestions during the final steps of manuscript preparation. The authors
359 of this manuscript declare no conflicts of interest. This work was supported by NIAID award
360 R01 AI110684 as well as by an American Cancer Society-Ellison Foundation Postdoctoral
361 Fellowship (PF-13-360-01-MPC), and a NIAID K22 Career Transition Award (1K22AI123465-
362 01).
363

363 **Figure Legends:**

364 **<u>Figure 1</u>: *ytfE* expression is regulated by NsrR and occurs within peripheral cells.** A)
365 C57BL/6 mice were inoculated intravenously (i.v.) with 10^3 WT *Y. pseudotuberculosis*, and
366 spleens were harvested at day 3 post-inoculation (PI). Bacterial transcripts were isolated from
367 splenic tissue, transcript levels were quantified by qRT-PCR relative to 16S, and the fold
368 increase in *ytfE* transcript levels is shown relative to the inoculum. Each dot represents an
369 individual mouse. B) Nitrogen stress was induced (NO_2, +) in cultures of WT and Δ*nsrR* strains,
370 and compared to untreated cultures (NO_2, -). The *ytfE* transcript levels are expressed relative to
371 16S, fold increase is relative to the average level in untreated WT cultures. Each column: 5
372 biological replicates, mean and SEM. C) C57BL/6 mice were inoculated i.v. with the WT
373 *hmp::mCherry ytfE::gfp* strain, and spleens were harvested at day 3 PI for fluorescence
374 microscopy. Fluorescent signal intensity was determined within the same peripheral and centroid
375 cells for *hmp* and *ytfE* reporters, and divided to generate the periphery/centroid ratio (4
376 mice/group). Dots: individual microcolonies. D) Representative image of *hmp::mCherry* and
377 *ytfE::gfp* reporters; merge and single channel images are shown. Statistics: Wilcoxon matched
378 pairs, **$p<0.01$, n.s.: not significant.

379

380 **<u>Figure 2</u>: *ytfE* contributes to growth in the spleen.** A) Co-infection with the WT and Δ*ytfE*
381 strains. C57BL/6 mice were inoculated i.v. with an equal mixture of $mCherry^+$ (*yopE::mCherry*)
382 WT and GFP^+ Δ*ytfE* strains, and spleens were harvested at day 3 PI. Competitive index: ratio of
383 Δ*ytfE*/WT CFUs in spleen at day 3, divided by ratio of Δ*ytfE*/WT CFUs in the inoculum. Dots:
384 individual mice. Dotted line: represents equal fitness. B) WT and Δ*ytfE* microcolony areas
385 (μm^2) from the co-infection quantified (Experimental Procedures) in 6 mice. C) C57BL/6 mice

386 were inoculated i.v. with the WT GFP$^+$ *hmp::mCherry* or Δ*ytfE* GFP$^+$ *hmp::mCherry* strains, and
387 spleens were harvested at day 3 PI for fluorescence microscopy. Reporter signals were
388 quantified within peripheral and centroid cells, *hmp* reporter signal was divided by GFP. D)
389 Representative image of a Δ*ytfE* GFP$^+$ *hmp::mCherry* microcolony, stained with Hoechst to
390 detect host nuclei; merge and *hmp* single channel images are shown Statistics: B): Mann-
391 Whitney, C): Wilcoxon matched pairs, ***p<0.001.
392
393 **Figure 3: Δ*hmp* Δ*ytfE* is attenuated for growth in the spleen.** A) C57BL/6 mice inoculated i.v.
394 with the WT GFP$^+$ or Δ*hmp* Δ*ytfE* GFP$^+$ strains, and spleens were harvested at day 3 PI to
395 quantify microcolony areas (μm^2) from single strain infections. Dots: individual microcolonies.
396 B) C57BL/6 mice were inoculated i.v. with an equal mixture of WT mCherry$^+$ (*yopE::mCherry*)
397 and Δ*hmp* Δ*ytfE* GFP$^+$ strains, and spleens were harvested at day 3 PI. Competitive index: ratio
398 of Δ*hmp* Δ*ytfE*/WT CFUs in spleen at day 3, divided by ratio of Δ*hmp* Δ*ytfE*/WT CFUs in the
399 inoculum. Dots: individual mice. Dotted line: represents equal fitness. C) WT and Δ*hmp* Δ*ytfE*
400 microcolony areas (μm^2) from the co-infection quantified (Experimental Procedures) in 7 mice.
401 Statistics: Mann-Whitney, *p<0.05.
402
403 **Figure 4: Δ*ytfE* contributes to survival in the absence of *hmp*.** A) C57BL/6 mice were
404 inoculated i.v. with an equal mixture of *hmp* GFP$^+$ and Δ*hmp* Δ*ytfE* GFP$^+$ P_{hmp}*::mCherry* strains,
405 and spleens were harvested at day 3 PI. Competitive index: ratio of Δ*hmp* Δ*ytfE*/Δ*hmp* CFUs in
406 spleen at day 3, divided by ratio of Δ*hmp* Δ*ytfE*/Δ*hmp* CFUs in the inoculum. Dots: individual
407 mice. Dotted line: represents equal fitness. B) Total CFUs in the spleen during co-infection,
408 when CI was less than 1 (Δ*hmp* wins) or above or equal to 1 (Δ*hmp* Δ*ytfE* wins). Dots: individual

409 mice. C) Δ*hmp* and Δ*hmp* Δ*ytfE* microcolony areas (μm^2) from the co-infection quantified
410 (Experimental Procedures) in 10 mice. Dots: individual microcolonies. D) Reporter signals were
411 quantified within peripheral and centroid cells in the Δ*hmp* Δ*ytfE* strain during co-infection, *hmp*
412 reporter signal was divided by GFP. Dots: individual microcolonies. Statistics: B) and C): Mann-
413 Whitney, D): Wilcoxon matched pairs, *p<0.05, **p<0.01, n.s.: not significant.
414
415 **<u>Figure 5</u>: YtfE activity is required in the absence of NO detoxification (Δ*hmp*).** A) Optical
416 density (A_{600nm}) was measured every 2 hours (time, hrs) within cultures of the indicated strains
417 during incubation in LB pH5.5 in the presence (+NO_2) and absence of $NaNO_2$. Data represents
418 two independent experiments. B) C57BL/6 mice were inoculated i.v. with the Δ*ytfE* GFP^+
419 P_{hmp}*::mCherry* or Δ*hmp* Δ*ytfE* GFP^+ P_{hmp}*::mCherry* strains, and spleens were harvested at day 3
420 PI for fluorescence microscopy. Reporter signals were quantified within peripheral and centroid
421 cells, *hmp* reporter signal was divided by GFP. Dots: individual microcolonies. C)
422 Representative images of Δ*ytfE* and Δ*hmp* Δ*ytfE* microcolonies; merge and *hmp* single channel
423 images are shown. Statistics: Wilcoxon matched pairs, *p<0.05, n.s.: not significant.
424
425 **<u>Figure 6:</u> Rescue of *ytfE* restores fitness of the Δ*ytfE* strain.** A) C57BL/6 mice were
426 inoculated i.v. with an equal mixture of *ytfE* rescued GFP^+ and WT $mCherry^+$ strains, and spleens
427 were harvested at day 3 PI. Competitive index: ratio of *ytfE* rescue/WT CFUs in spleen at day 3,
428 divided by ratio of *ytfE* rescue/WT CFUs in the inoculum. Dots: individual mice. Dotted line:
429 represents equal fitness. B) WT and *ytfE* rescue microcolony areas (μm^2) from the co-infection
430 quantified (Experimental Procedures) in 10 mice. Dots: individual microcolonies. C)
431 Representative images of WT $mCherry^+$ and *ytfE* rescued GFP^+ microcolonies. Scale bar: 20μm.

432 Statistics: Mann-Whitney, n.s.: not significant.

433 **References**

434 1. Bogdan C. Nitric oxide and the immune response. Nat Immunol. 2001;2(10):907-16.

435 2. Nathan C. Nitric oxide as a secretory product of mammalian cells. FASEB J.
436 1992;6(12):3051-64.

437 3. Pervin S, Singh R, Hernandez E, Wu G, Chaudhuri G. Nitric oxide in physiologic
438 concentrations targets the translational machinery to increase the proliferation of human breast
439 cancer cells: involvement of mammalian target of rapamycin/eIF4E pathway. Cancer Res.
440 2007;67(1):289-99.

441 4. Pervin S, Singh R, Chaudhuri G. Nitric oxide-induced cytostasis and cell cycle arrest of a
442 human breast cancer cell line (MDA-MB-231): potential role of cyclin D1. Proc Natl Acad Sci.
443 2001;98(6):3583-8.

444 5. Dubey M, Nagarkoti S, Awasthi D, Singh A, Chandra T, Kumaravelu J, et al. Nitric
445 oxide-mediated apoptosis of neutrophils through caspase-8 and caspase-3-dependent mechanism.
446 Cell Death Dis. 2016;7(9):e2348.

447 6. Kumar S, Barthwal M, Dikshit M. Cdk2 nitrosylation and loss of mitochondrial potential
448 mediate NO-dependent biphasic effect on HL-60 cell cycle. Free Radic Biol Med.
449 2010;48(6):851-61.

450 7. Kobayashi Y. The regulatory role of nitric oxide in proinflammatory cytokine expression
451 during the induction and resolution of inflammation. J Leukoc Biol. 2010;88(6):1157-62.

452 8. Zeigler M, Doseff A, Galloway M, Opalek J, Nowicki P, Zweier J, et al. Presentation of
453 nitric oxide regulates monocyte survival through effects on caspase-9 and caspase-3 activation. J
454 Biol Chem. 2003;278(15):12894-902.

455 9. Pautz A, Art J, Hahn S, Nowag S, Voss C, Kleinert H. Regulation of the expression of
456 inducible nitric oxide synthase. Nitric Oxide. 2010;23(2):75-93.

457 10. Pullan S, Gidley M, Jones R, Barrett J, Stevanin T, Read R, et al. Nitric oxide in
458 chemostat-cultured *Escherichia col*i is sensed by Fnr and other global regulators: unaltered
459 methionine biosynthesis indicates lack of S nitrosation. J Bacteriol. 2007;189(5):1845-55.

460 11. Gilberthorpe N, Lee M, Stevanin T, Read R, Poole R. NsrR: a key regulator
461 circumventing *Salmonella enterica* serovar Typhimurium oxidative and nitrosative stress *in vitro*
462 and in IFN-gamma-stimulated J774.2 macrophages. Microbiology. 2007;153(6):1756-71.

463 12. Overton T, Justino M, Li Y, Baptista J, Melo A, Cole J, et al. Widespread distribution in
464 pathogenic bacteria of di-iron proteins that repair oxidative and nitrosative damage to iron-sulfur
465 clusters. J Bacteriol. 2008;190(6):2004-13.

466 13. Bodenmiller D, Spiro S. The *yjeB* (*nsrR*) gene of *Escherichia coli* encodes a nitric oxide-
467 sensitive transcriptional regulator. J Bacteriol. 2006;188(3):874-81.

468 14. Tucker N, Hicks M, Clarke T, Crack J, Chandra G, Le Brun N, et al. The transcriptional
469 repressor protein NsrR senses nitric oxide directly via a [2Fe-2S] cluster. PLoS ONE.
470 2008;3(11):e3623.

471 15. Volbeda A, Dodd E, Darnault C, Crack J, Renoux O, Hutchings M, et al. Crystal
472 structures of the NO sensor NsrR reveal how its iron-sulfur cluster modulates DNA binding. Nat
473 Commun. 2017;8:15052.

474 16. Filenko N, Spiro S, Browning D, Squire D, Overton T, Cole J, et al. The NsrR regulon of
475 *Escherchia coli* K-12 includes genes encoding the hybrid cluster protein and the periplasmic,
476 respiratory nitrite reductase. J Bacteriol. 2007;189(12):4410-7.

477 17. Partridge J, Bodenmiller D, Humphrys M, Spiro S. NsrR targets in the *Escherchia coli*
478 genome: new insights into DNA sequence requirements for binding and a role for NsrR in the
479 regulation of motility. Mol Microbiol. 2009;73(4):680-94.

480 18. Robinson J, Brynildsen M. A kinetic platform to determine the fate of nitric oxide in
481 *Escherichia coli*. PLoS Comput Biol. 2013;9(5):e103049.

482 19. Poole R, Anjum M, Membrillo-Hernández J, Kim S, Hughes M, Stewart V. Nitric oxide,
483 nitrite, and Fnr regulation of *hmp* (flavohemoglobin) gene expression in *Escherichia coli* K-12. J
484 Bacteriol. 1996;178(18):5487-92.

485 20. Justino M, Almeida C, Gonçalves V, Teixeira M, Saraiva L. *Escherichia coli* YtfE is a
486 di-iron protein with an important function in assembly of iron-sulphur clusters. FEMS Microbiol
487 Lett. 2006;257(2):278-84.

488 21. Todorovic S, Justino M, Wellenreuther G, Hildebrandt P, Murgida D, Meyer-Klaucke W,
489 et al. Iron-sulfur repair YtfE protein from *Escherichia coli*: structural characterization of the di-
490 iron center. J Biol Inorg Chem. 2008;13(5):765-70.

491 22. Miller H, Kwuan L, Schwiesow L, Bernick D, Mettert E, Ramirez H, et al. IscR is
492 essential for *Yersinia pseudotuberculosis* type III secretion and virulence. PLoS Pathog.
493 2014;10(6):e1004194.

494 23. Miller H, Schwiesow L, Au-Yeung W, Auerbuch V. Hereditary hemochromatosis
495 predisposes mice to *Yersinia pseudotuberculosis* infection even in the absence of the type III
496 secretion system. Front Cell Infect Microbiol. 2016;6:69.

497 24. Schwiesow L, Mettert E, Wei Y, Miller H, Herrera N, Balderas D, et al. Control of *hmu*
498 heme uptake genes in *Yersinia pseudotuberculosis* in response to iron sources. Front Cell Infect
499 Microbiol. 2018;8:47.

500 25. Hubbert W, Petenyi C, Glasgow L, Uyeda C, Creighton S. *Yersinia pseudotuberculosis*
501 infection in the United States. Septicemia, appendicitis, and mesenteric lymphadenitis. Am J
502 Trop Med Hyg. 1971;20(5):679-84.

503 26. Gurry J. Acute terminal ileitis and *Yersinia* infection. Br Med J. 1974;2(5913):264-6.

504 27. Capron J, Delamarre J, Delcenserie R, Gineston J, Dupas J, Lorriaux A. Liver absess
505 complicating *Yersinia pseudotuberculosis* ileitis. Gastroenterology. 1981;81(1):150-2.

506 28. Paff J, Triplett D, Saari T. Clinical and laboratory aspects of *Yersinia pseudotuberculosis*
507 infections, with a report of two cases. Am J Clin Pathol. 1976;66(1):101-10.

508 29. Barnes P, Bergman M, Mecsas J, Isberg R. *Yersinia pseudotuberculosis* disseminates
509 directly from a replicating bacterial pool in the intestine. J Exp Med. 2006;203(6):1591-601.

510 30. Crimmins G, Mohammadi S, Green E, Bergman M, Isberg R, Mecsas J. Identification of
511 MrtAB, an ABC transporter specifically required for *Yersinia pseudotuberculosis* to colonize the
512 mesenteric lymph nodes. PLoS Pathog. 2012;8(8):e1002828.

513 31. Davis K, Mohammadi S, Isberg R. Community behavior and spatial regulation within a
514 bacterial microcolony in deep tissue sites serves to protect against host attack. Cell Host
515 Microbe. 2015;17(1):21-31.

516 32. Zhang Y, Khairallah C, Sheridan B, van der Velden A, Bliska J. CCR2+ inflammatory
517 monocytes are recruited to *Yersinia pseudotuberculosis* pyogranulomas and dictate adaptive
518 responses at the expense of innate immunity during oral infection. Infect Immun.
519 2018;86(3):e00782-17.

520 33. Peterson L, Philip N, DeLaney A, Wynosky-Dolfi M, Asklof K, Gray F, et al. RIPK1-
521 dependent apoptosis bypasses pathogen blockage of innate signaling to promote immune
522 defense. J Exp Med. 2017;214(11):3171-82.

523 34. Durand E, Maldonado-Arocho F, Castillo C, Walsh R, Mecsas J. The presence of
524 professional phagocytes dictates the number of host cells targeted for Yop translocation during
525 infection. Cell Microbiol. 2010;12(8):1064-82.

526 35. Sebbane F, Lemaître N, Sturdevant D, Rebeil R, Virtaneva K, Porcella S, et al. Adaptive
527 response of *Yersinia pestis* to extracellular effectors of innate immunity during bubonic plague.
528 Proc Natl Acad Sci. 2006;103(31):11766-71.

529 36. Karlinsey J, Bang I, Becker L, Frawley E, Porwollik S, Robbins H, et al. The NsrR
530 regulon in nitrosative stress resistance of *Salmonella enterica* serovar Typhimurium. Mol
531 Microbiol. 2012;85(6):1179-93.

532 37. Shepherd M, Achard M, Idris A, Totsika M, Phan M, Peters K, et al. The cytochrome bd-
533 I respiratory oxidase augments survival of multidrug-resistant *Escherichia coli* during infection.
534 Sci Rep. 2016;6:35285.

535 38. Shiloh M, MacMicking J, Nicholson S, Brause J, Potter S, Marino M, et al. Phenotype of
536 mice and macrophages deficient in both phagocyte oxidase and inducible nitric oxide synthase.
537 Immunity. 1999;10(1):29-38.

538 39. Vasquez-Torres A, Jones-Carson J, Mastroeni P, Ischiropoulos H, Fang F. Antimicrobial
539 actions of the NADPH phagocyte oxidase and inducible nitric oxide synthase in experimental
540 salmonellosis. I. Effects on microbial killing by activated peritoneal macrophages *in vitro*. J Exp
541 Med. 2000;192(2):227-36.

542 40. Shiloh M, Nathan C. Reactive nitrogen intermediates and the pathogenesis of *Salmonella*
543 and *Mycobacteria*. Curr Opin Microbiol. 2000;3(1):35-42.

544 41. Bang I, Liu L, Vasquez-Torres A, Crouch M, Stamler J, Fang F. Maintenance of nitric
545 oxide and redox homeostasis by the *Salmonella* flavohemoglobin *hmp*. J Biol Chem.
546 2006;281(38):28039-47.

547 42. Mashruwala A, Boyd J. The *Staphylococcus aureus* SrrAB regulatory system modulates
548 hydrogen peroxide resistance factors, which imparts protection to aconitase during aerobic
549 growth. PLoS ONE. 2017;12(1):e0170283.

550 43. Djaman O, Outten F, Imlay J. Repair of oxidized iron-sulfur clusters in *Escherchia coli*. J
551 Biol Chem. 2004;279(43):44590-99.

552 44. Nuss A, Beckstette M, Pimenova M, Schmühl C, Opitz W, Pisano F, et al. Tissue dual
553 RNA-seq allows fast discovery of infection-specific functions and riboregulators shaping host-
554 pathogen transcriptomes. Proc Natl Acad Sci. 2017;114(5):E791-E800.

555 45. Justino M, Almeida C, Teixeira M, Saraiva L. *Escherichia coli* di-iron YtfE protein is
556 necessary for the repair of stress-damaged iron-sulfur clusters. J Biol Chem.
557 2007;282(14):10352-9.
558
559

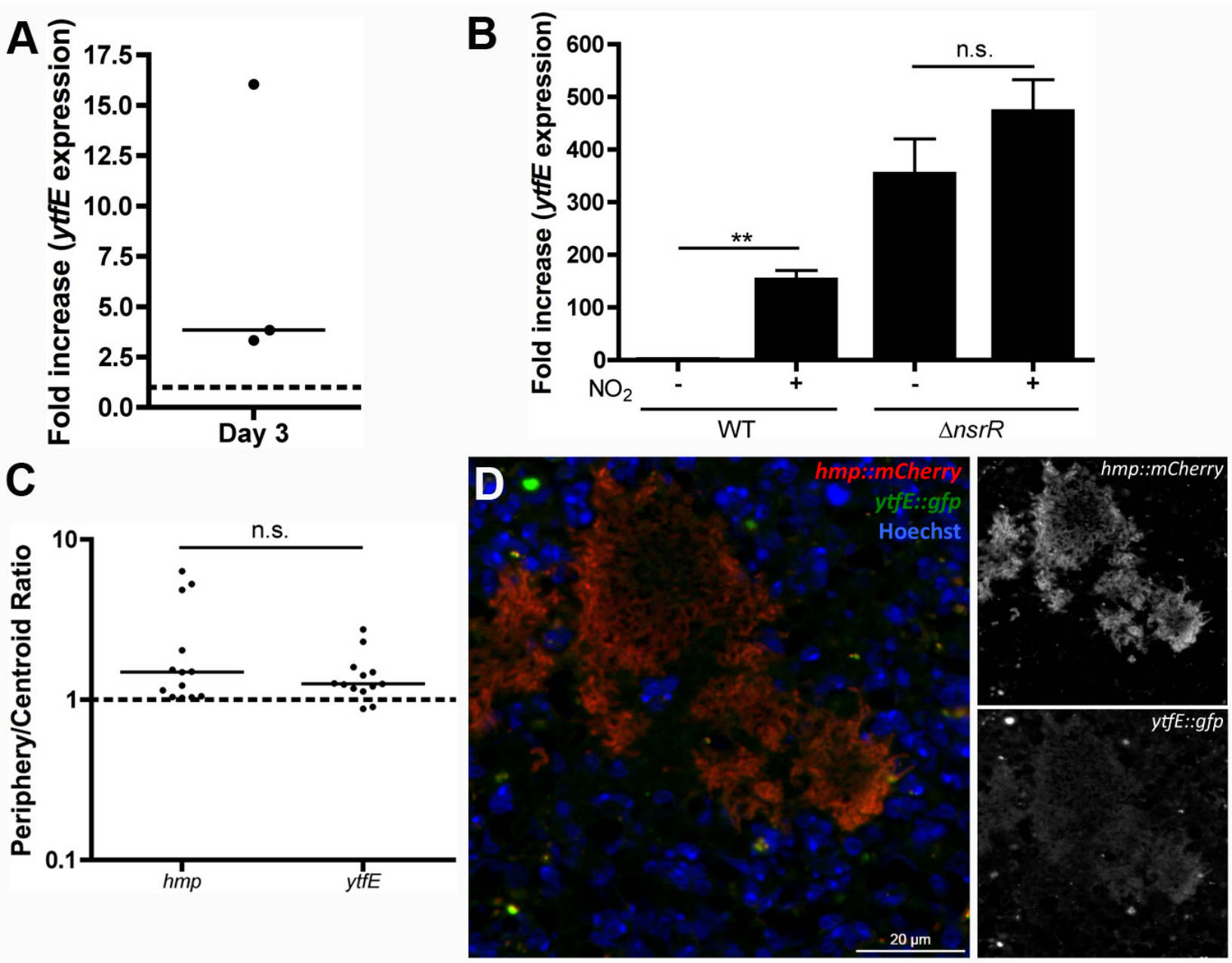
A
Fold increase (ytfE expression)
17.5
15.0
12.5
10.0
7.5
5.0
2.5
0.0
Day 3
B
Fold increase (ytfE expression)
600
500
400
300
200
100
0
n.s.
**
NO2
-
+
-
+
WT
ΔnsrR
C
Periphery/Centroid Ratio
10
1
0.1
n.s.
hmp
ytfE
D
hmp::mCherry
ytfE::gfp
Hoechst
20 µm
hmp::mCherry
ytfE::gfp

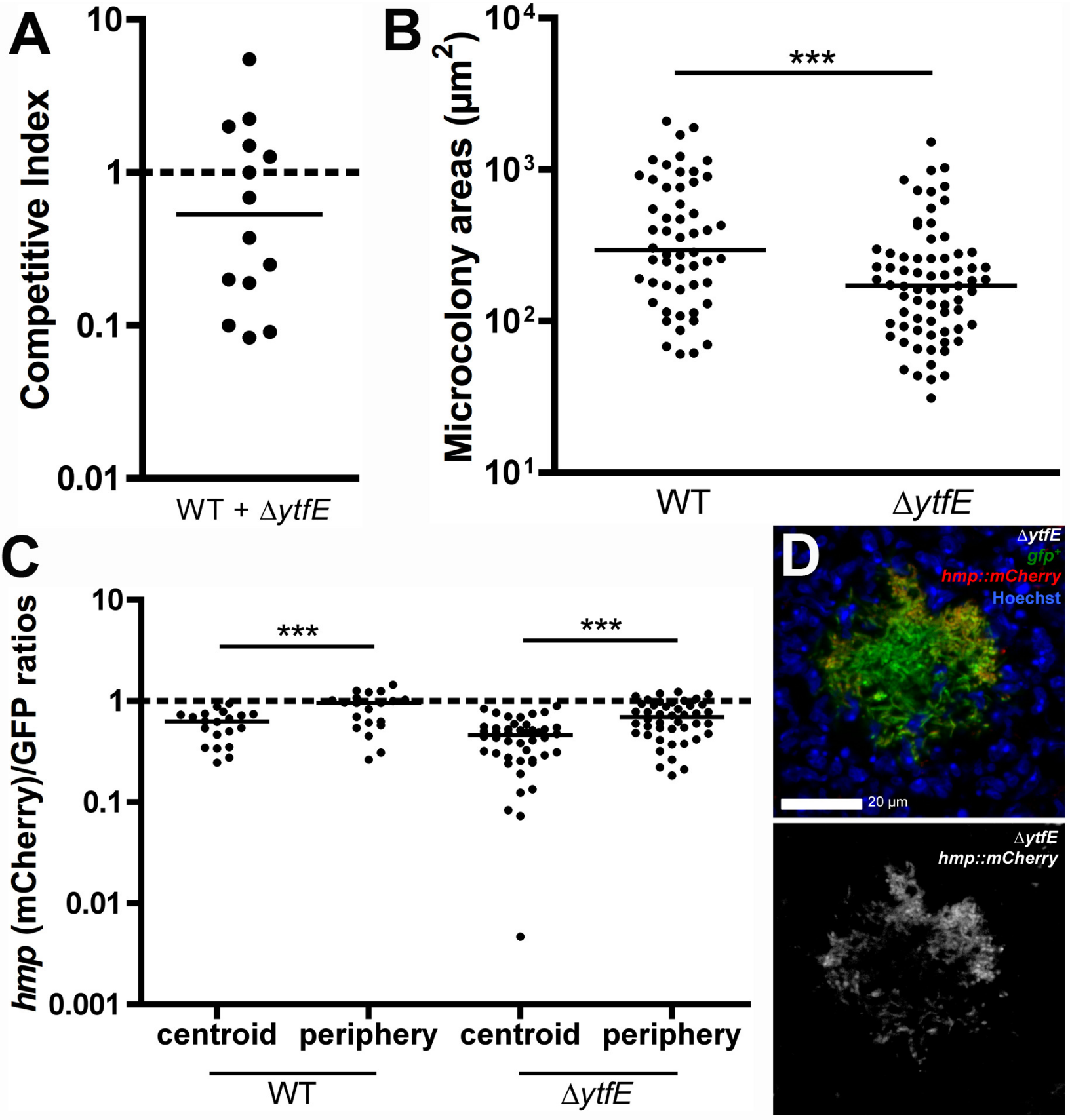
A
Competitive Index
10
1
0.1
0.01
WT + ΔytfE
B
Microcolony areas (μm²)
10⁴
10³
10²
10¹
***
WT
ΔytfE
C
hmp (mCherry)/GFP ratios
10
1
0.1
0.01
0.001
***
***
centroid
periphery
centroid
periphery
WT
ΔytfE
D
ΔytfE
gfp+
hmp::mCherry
Hoechst
20 μm
ΔytfE
hmp::mCherry

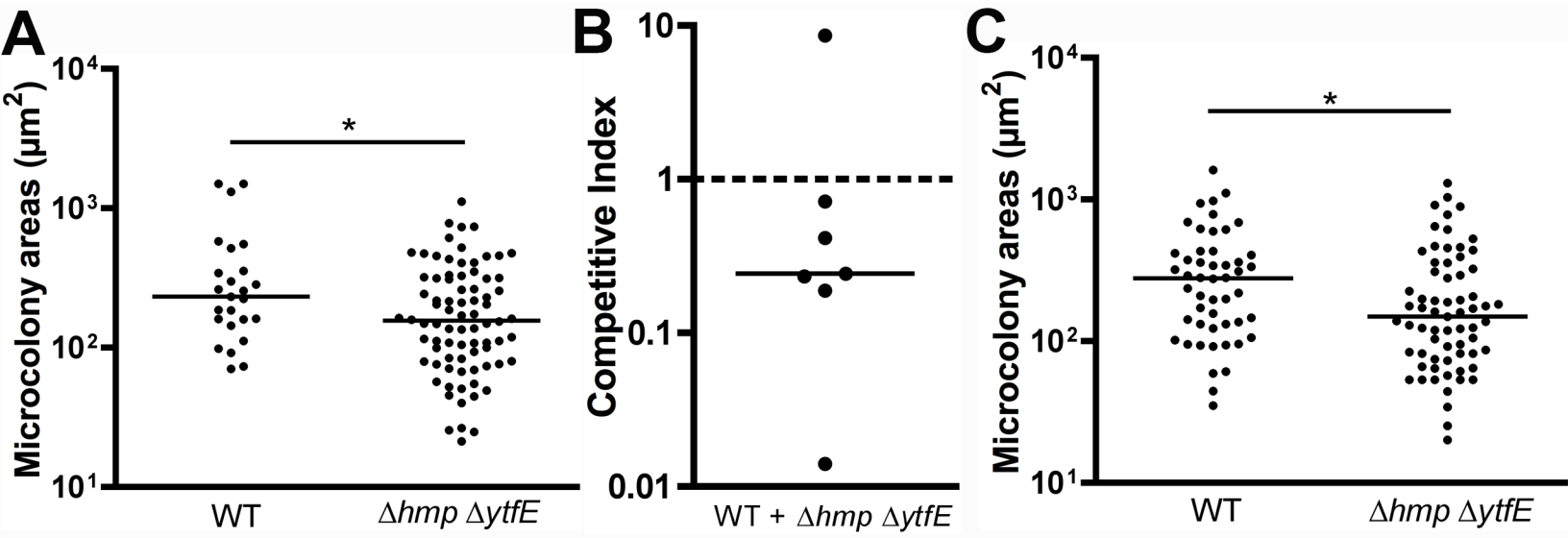
A
Microcolony areas (μm²)
10⁴
10³
10²
10¹
*
WT
Δhmp ΔytfE
B
Competitive Index
10
1
0.1
0.01
WT + Δhmp ΔytfE
C
Microcolony areas (μm²)
10⁴
10³
10²
10¹
*
WT
Δhmp ΔytfE

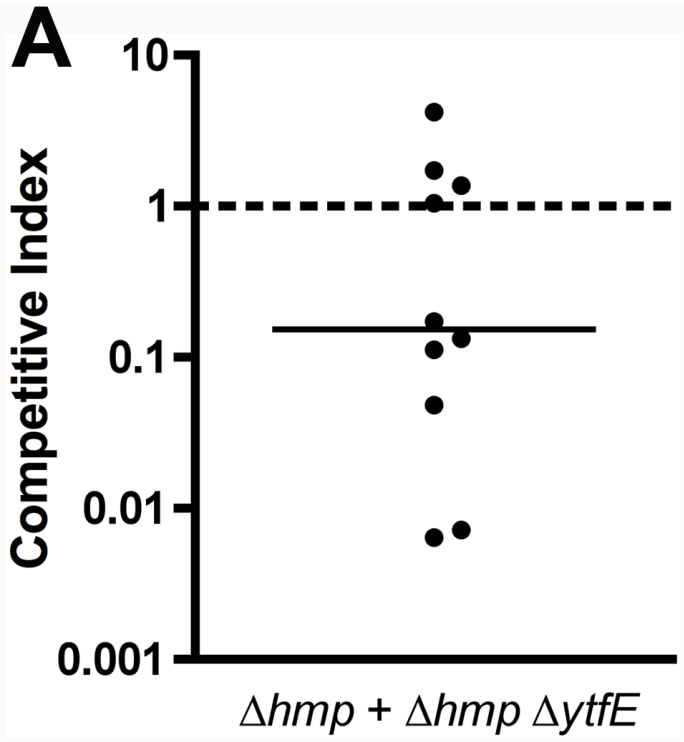
A
Competitive Index
10
1
0.1
0.01
0.001
Δhmp + Δhmp ΔytfE

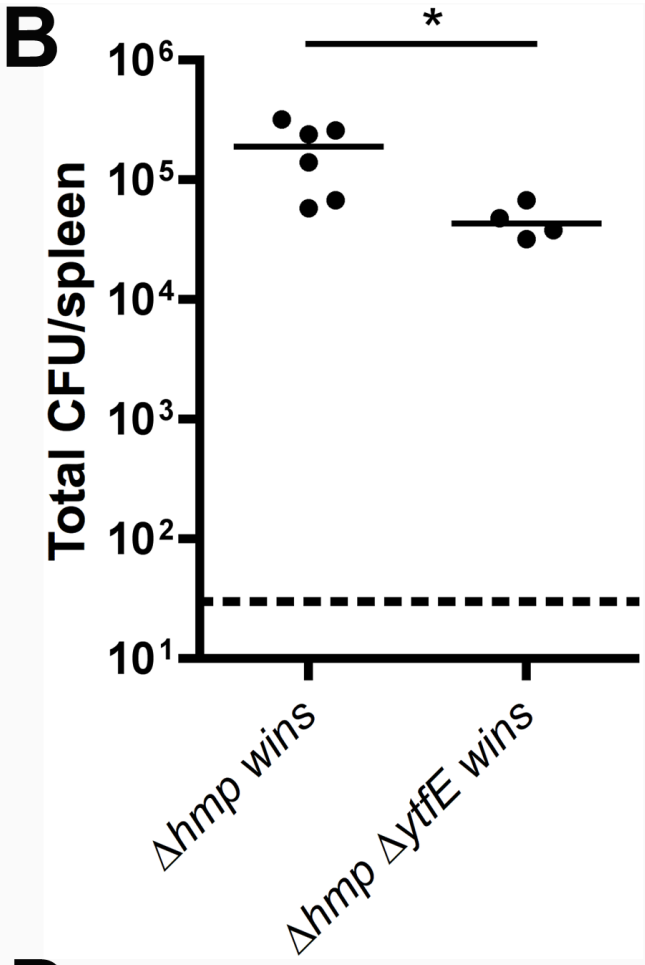
B
*
Total CFU/spleen
10^6
10^5
10^4
10^3
10^2
10^1
Δhmp wins
Δhmp ΔytfE wins

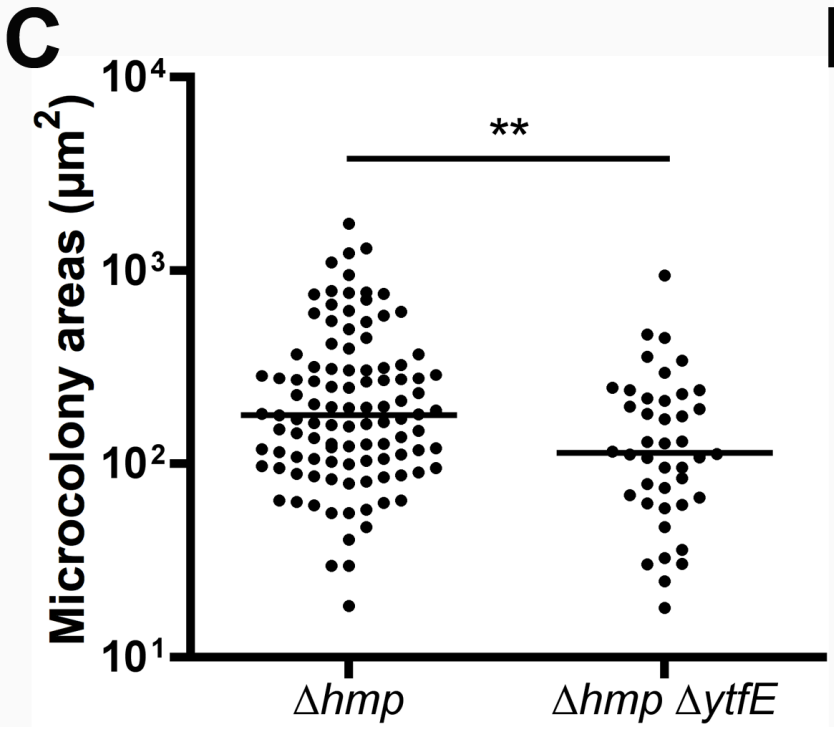
C
**
Microcolony areas (μm^2)
10^4
10^3
10^2
10^1
Δhmp
Δhmp ΔytfE

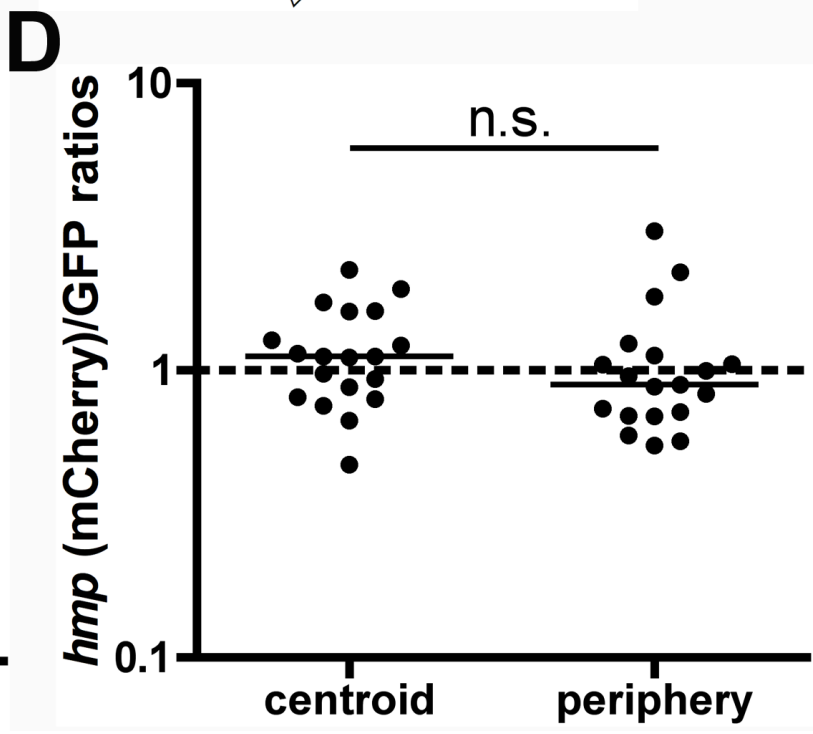
D
n.s.
hmp (mCherry)/GFP ratios
10
1
0.1
centroid
periphery

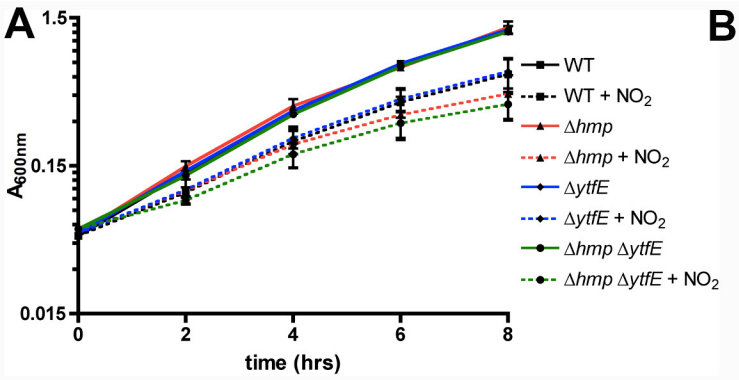
A
1.5
0.15
0.015
A_{600nm}
0
2
4
6
8
time (hrs)
WT
WT + NO_2
Δhmp
Δhmp + NO_2
ΔytfE
ΔytfE + NO_2
Δhmp ΔytfE
Δhmp ΔytfE + NO_2

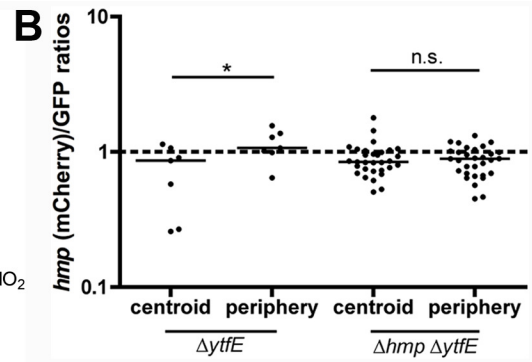
B
10
1
0.1
hmp (mCherry)/GFP ratios
*
n.s.
centroid
periphery
centroid
periphery
ΔytfE
Δhmp ΔytfE

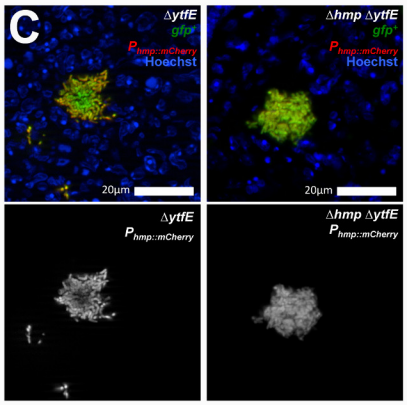
C
ΔytfE
gfp+
$P_{hmp::mCherry}$
Hoechst
20μm
Δhmp ΔytfE
gfp+
$P_{hmp::mCherry}$
Hoechst
20μm
ΔytfE
$P_{hmp::mCherry}$
Δhmp ΔytfE
$P_{hmp::mCherry}$

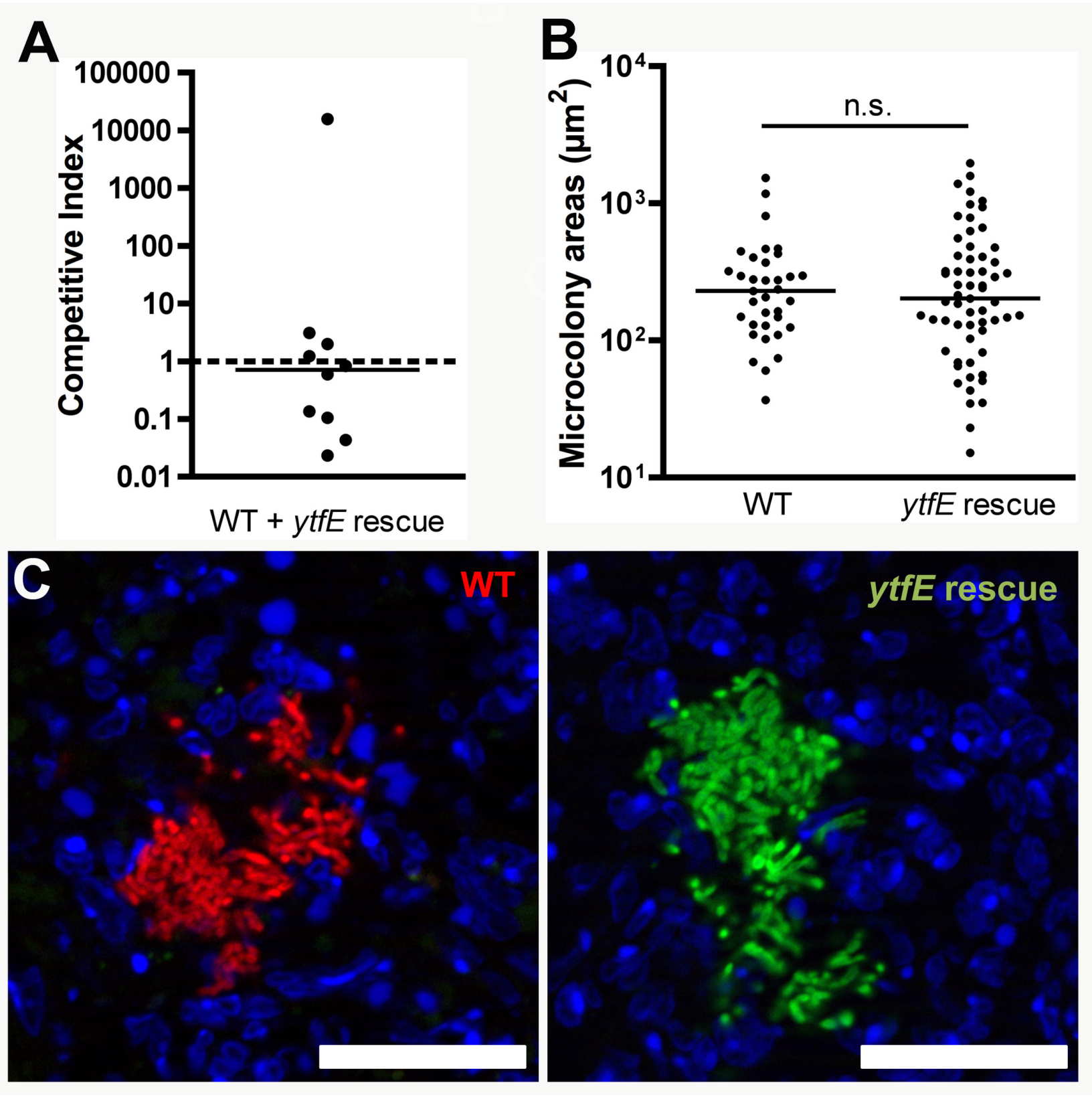
A
Competitive Index
100000
10000
1000
100
10
1
0.1
0.01
WT + ytfE rescue
B
Microcolony areas (μm2)
10^4
10^3
10^2
10^1
n.s.
WT
ytfE rescue
C
WT
ytfE rescue